

RESEARCH ARTICLE

Cerebral oxygen metabolism in adults with sickle cell disease

Lena Václavú^{1,2}  | Jan Petr³ | Esben Thade Petersen^{4,5} |
Henri J.M.M. Mutsaerts⁶ | Charles B.L. Majoie¹ | John C. Wood⁷ | Ed VanBavel⁸ |
Aart J. Nederveen¹ | Bart J. Biemond⁹

¹Radiology & Nuclear Medicine, Amsterdam UMC, University of Amsterdam, Amsterdam, The Netherlands

²C.J. Gorter Center for High Field MRI, Department of Radiology, Leiden University Medical Center, Leiden University, Leiden, The Netherlands

³Helmholtz-Zentrum Dresden-Rossendorf, Institute of Radiopharmaceutical Cancer Research, Dresden, Germany

⁴Danish Research Centre for Magnetic Resonance, Centre for Functional and Diagnostic Imaging and Research, Copenhagen University Hospital Hvidovre, Hvidovre, Denmark

⁵Center for Magnetic Resonance, Department of Health Technology, Technical University of Denmark, Kongens Lyngby, Denmark

⁶Radiology & Nuclear Medicine, Amsterdam UMC, Vrije Universiteit, Amsterdam, The Netherlands

⁷Cardiology & Radiology, Children's Hospital of Los Angeles, Los Angeles, California

⁸Biomedical Engineering & Physics, Amsterdam UMC, University of Amsterdam, Amsterdam, The Netherlands

⁹Hematology, Amsterdam UMC, University of Amsterdam, Amsterdam, The Netherlands

Correspondence

Lena Václavú, Department of Radiology, Leiden University Medical Center, Leiden University, Leiden, The Netherlands.
Email: l.vaclavu@lumc.nl

Abstract

In sickle cell disease (SCD), oxygen delivery is impaired due to anemia, especially during times of increased metabolic demand, and cerebral blood flow (CBF) must increase to meet changing physiologic needs. But hyperemia limits cerebrovascular reserve (CVR) and ischemic risk prevails despite elevated CBF. The cerebral metabolic rate of oxygen (CMRO₂) directly reflects oxygen supply and consumption and may therefore be more insightful than flow-based CVR measures for ischemic risk in SCD. We hypothesized that adults with SCD have impaired CMRO₂ at rest and that a vasodilatory challenge with acetazolamide would improve CMRO₂. CMRO₂ was calculated from CBF and oxygen extraction fraction (OEF), measured with arterial spin labeling and T₂-prepared tissue relaxation with inversion recovery (T₂-TRIR) MRI. We studied 36 adults with SCD without a clinical history of overt stroke, and nine healthy controls. As expected, CBF was higher in patients with SCD versus controls (mean ± SD: 74 ± 16 versus 46 ± 5 mL/100 g/min, *P* < .001), resulting in similar oxygen delivery (SCD: 377 ± 67 versus controls: 368 ± 42 μmol O₂/100g/min, *P* = .69). OEF was lower in patients versus controls (27 ± 4 versus 35 ± 4%, *P* < .001), resulting in lower CMRO₂ in patients versus controls (102 ± 24 versus 127 ± 20 μmol O₂/100g/min, *P* = .002). After acetazolamide, CMRO₂ declined further in patients (*P* < .01) and did not decline significantly in controls (*P* = .78), indicating that forcing higher CBF worsened oxygen utilization in SCD patients. This lower CMRO₂ could reflect variation between healthy and unhealthy vascular beds in terms of dilatory capacity and resistance whereby dysfunctional vessels become more oxygen-deprived, hence increasing the risk of localized ischemia.

1 | INTRODUCTION

Sickle cell disease (SCD) is caused by a genetic mutation whereby sickle hemoglobin (*HbS*) polymerizes in its deoxygenated form, leading to impaired oxygen transport and chronic hemolytic anemia. In SCD,

acute anemia increases the risk for silent cerebral infarcts (SCI),¹⁻³ despite elevated cerebral blood flow (CBF) to compensate anemia.⁴⁻⁶ Interruptions to CBF are associated with ischemic risk,⁷ and MRI studies have shown a high prevalence of SCI in both children and adults with SCD.⁸ While overt stroke is preventable with transfusion

This is an open access article under the terms of the Creative Commons Attribution-NonCommercial-NoDerivs License, which permits use and distribution in any medium, provided the original work is properly cited, the use is non-commercial and no modifications or adaptations are made.

© 2020 The Authors. *American Journal of Hematology* published by Wiley Periodicals, Inc.

therapy,⁹ SCI still remain poorly understood, and advances in MR technology are becoming more instrumental in our investigation of SCI development and progression in SCD.¹⁰ For instance, SCIs are associated with cognitive impairment and lesion progression in adults with SCD,¹¹⁻¹³ and indicate that the balance between oxygen demand and delivery, which serves to maintain cerebral metabolism, may be disrupted.

The cerebral metabolic rate of oxygen (CMRO₂) quantitatively describes the rate of oxygen consumption by metabolic processes in cerebral tissue. The CMRO₂ is high in healthy children to meet the metabolic demands of the developing brain, particularly between the ages of 2 and 10 years,¹⁴ which is also the age range in which overt stroke has the highest incidence in SCD.^{9,15} Hence, CBF can be particularly high in children with SCD in whom anemia and metabolic requirements play an additive role in increasing blood flow and associated increased risk of overt stroke.^{16,17} Note that CMRO₂ typically declines with age^{18,19} and CBF matches oxygen delivery to this change in metabolic demand.²⁰ Oxygen extraction fraction (OEF) measured by MRI can serve as a non-invasive measure of the efficacy of oxygen supply-demand mechanisms.²⁰ Studies in adult patients with SCD have varied in their methods and conclusions as to whether CMRO₂ is maintained in the presence of chronic demands on CBF to counteract anemia.²¹⁻²³

In SCD, cerebrovascular reserve is reduced,²⁴⁻²⁶ in particular, CBF may already be maximally recruited for basal oxygen demands and might even be unable to maintain the required CMRO₂ in periods of increased metabolic needs. This infers a risk of insufficient oxygen in acute anemic periods,¹ particularly to regions where CBF is already relatively low.²⁷⁻²⁹ Recent work shows that oxygen metabolism could actually decrease if CBF increases in the presence of capillary transit time heterogeneity (CTH).³⁰ A potential effect offsetting this microvascular shunting is that anemia induces a rightward shift in oxygen-dissociation, allowing more efficient oxygen diffusion in SCD. While these opposing processes are challenging to disentangle, and may cancel out, we tested the hypothesis that CMRO₂ is reduced in adult patients with SCD as a result of chronic anemia and impaired vascular reserve capacity, which may also explain the high prevalence of (silent) cerebral infarcts in this population.³¹ The second hypothesis was that vasodilation can improve CMRO₂ by generating an increase in blood and oxygen flow. Accordingly, the aim of this study was to examine CMRO₂ using specialized MRI techniques³²⁻³⁴ in adults with SCD without a clinical history of stroke, and to measure the response to vasodilation with acetazolamide^{35,36} to better understand the etiology of ischemic risk in these patients.

2 | METHODS

2.1 | Participants

This cross-sectional study was approved by the local Institutional Review Board (IRB) at the Amsterdam University Medical Centers (Amsterdam UMC, Location AMC) in The Netherlands, and carried out in accordance with the Declaration of Helsinki. This study was

registered at clinicaltrials.gov under the ID: NCT02824406. All participants provided informed consent prior to study participation. Inclusion criteria were adults (>18 years) with SCD (*HbSS* or *HbSβ⁰*-thalassaemia) recruited from the outpatient clinic at the Amsterdam UMC. Age-, sex-, and race-matched healthy controls were recruited from friends and relatives of the participating patients. Exclusion criteria were contraindications to MRI and acetazolamide, and a clinical history of stroke, a cerebrovascular accident or neurologic disease affecting cerebral autoregulation. Additionally, patients were in steady state at the time of the MRI examination. Steady state was defined as no infection or hospitalization for a painful crisis in the month prior to participation. The cohort has previously been described in Václavů et al.²⁶ One patient was receiving blood transfusions for prevention of stroke upon detection of high TCD values while still in pediatric care, and two other patients were on transfusions for prevention of frequent hydroxyurea refractory vaso-occlusive crises/acute chest syndrome.

2.2 | Blood markers

Blood samples were drawn from an antecubital vein in all participants, and an intravenous catheter was placed at the site of cannulation directly prior to MRI for acetazolamide administration during the scan. Genotype (*HbAA*, *HbAS*, *HbSS* or *HbSβ⁰*) was confirmed with high performance liquid chromatography (HPLC) and DNA analysis. The following parameters were analyzed for their association with CMRO₂: hemoglobin (Hb) hematocrit (Hct), MCV, leukocyte and platelet counts, *HbS*% and fetal hemoglobin (*HbF* %), creatinine, ASAT, ALAT, and plasma ferritin levels. Surrogate markers for hemolysis were defined as LDH, reticulocytes, and bilirubin levels.

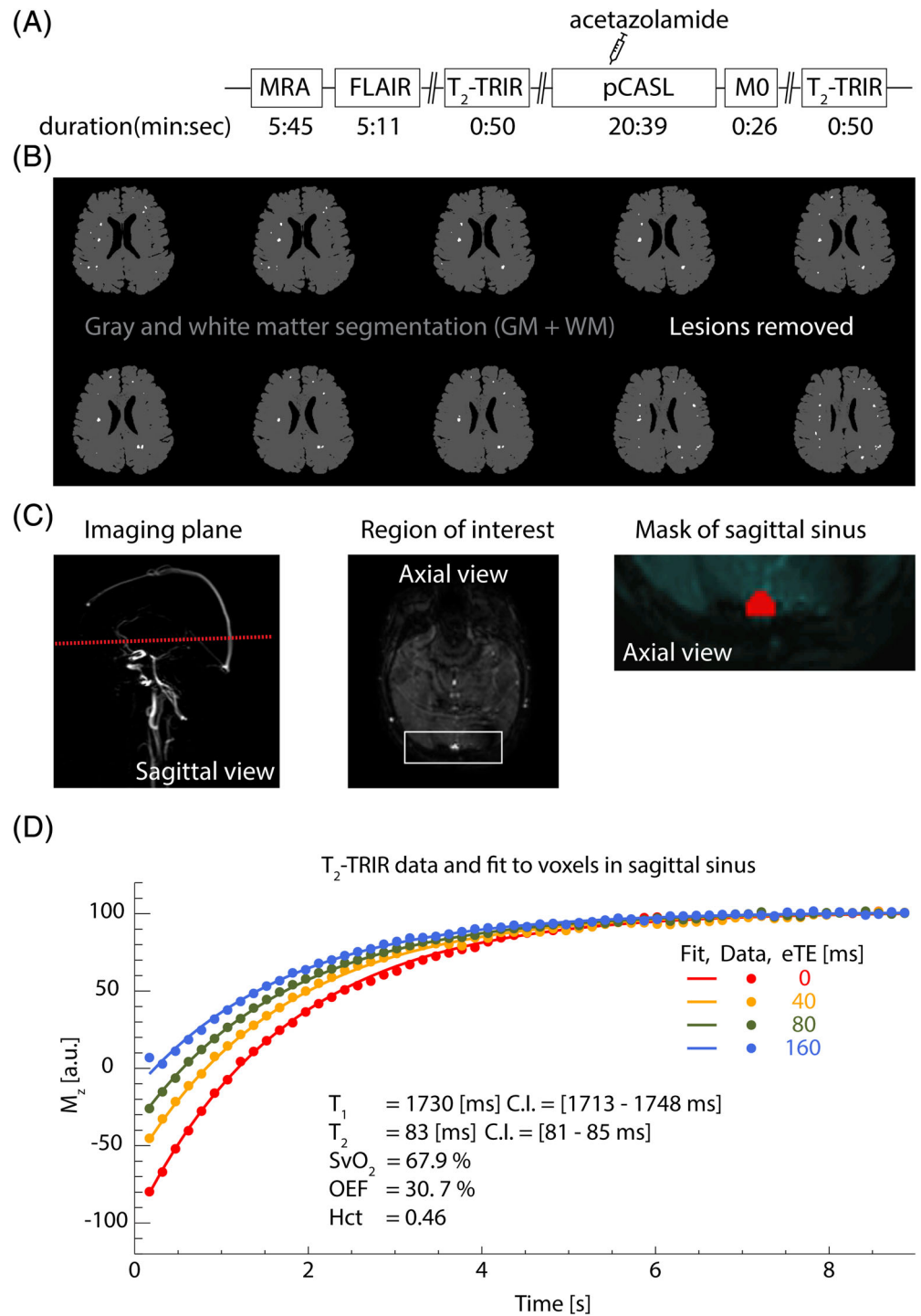
2.3 | MR imaging

All images were acquired on a 3 T Ingenia clinical MR system (Philips Healthcare, Best, The Netherlands) using a 32-channel receive head-coil and body-coil transmission. The MRI protocol is depicted in Figure 1A, and comprised MR angiography (MRA) for vasculopathy, fluid-attenuated inversion recovery (FLAIR) for anatomy and lesions, T₂-prepared tissue relaxation with inversion recovery (T₂-TRIR) for venous blood oxygen saturation and T₁ of blood, and pseudo continuous arterial spin labelling (pCASL) for cerebral blood flow.

Lesions and brain volume were assessed using a high resolution T₂-weighted 3D multi-shot TSE fluid attenuated inversion recovery (FLAIR) sequence with a FOV 250 x 250 x 180 mm, voxel size 0.98 x 0.98 x 1.12 mm, TR/TE 4800/356 ms, SENSE acceleration factor AP/FH 2.6/2, SPAIR fat suppression, inversion delay 1650 ms, flip angle 90° and scan duration of 5:11 minutes.

Vasculopathy was assessed in maximum intensity projection reconstructions of right-left and feet-head projections and in magnitude images of non-contrast enhanced 3D T₁ time-of-flight FFE RF-spoiled gradient echo inflow angiography MRA (TR/TE 21/4 ms, FOV 200 x 200 x 90 mm, voxel size 0.39 x 0.39 x 0.5 mm, flip angle 20°, 180 axial slices, scan duration 5:45 minutes).

FIGURE 1 MRI procedures. A, The sequence started with an MRA and FLAIR scan for vasculopathy, anatomy and lesions, followed by a baseline T_2 measurement (T_2 -TRIR), and baseline pseudo-continuous arterial spin labelling (pCASL) scan during which acetazolamide was administered intravenously. The T_2 measurement was repeated 25 minutes after the injection. B, A mask for cerebral blood flow (CBF) was obtained from the segmented gray matter (GM) and white matter (WM) tissue volumes with lesions removed. C, Measurement of the T_2 -TRIR plane is shown in as a red line representing perpendicular placement to the sagittal sinus. The sagittal sinus was detected automatically (shown in red) and the fit was initiated in the voxels contained in this mask. D, The data points and fit of the average of the voxels from one participant is shown for T_1 of all the effective echo times (eTE, 0, 40, 80, and 160 ms). Essentially, the T_2 decay curve can be obtained from any four points (four eTEs) belonging to each time point along the x-axis, but to increase the robustness the T_2 curve was fitted simultaneously with the T_1 curve in all acquired time points using a least squares minimizing function [Color figure can be viewed at wileyonlinelibrary.com]



Venous blood T_1 and T_2 were simultaneously measured in the sagittal sinus with a T_2 -TRIR sequence consisting of a global slab-selective frequency offset corrected inversion (FOCI) pulse and T_2 preparation preceding a single slice 2D single-shot FFE EPI Look-Locker read-out.^{33,34,37} The parameters of the T_2 -TRIR were FOV 202 x 243 mm, voxel size 1.69 x 1.69 x 4 mm, 1 transverse slice placed perpendicular to the posterior sagittal sinus, TR/TE 150/24 ms, SENSE acceleration factor AP 3, and four T_2 weightings resulting in effective echo times (eTE) of 0, 40, 80, and 160 ms. This corresponded to 0, 4, 8 and 16 refocusing pulses in the MLEV T_2 -preparation with a Carr-Purcell- Meiboom-Gill

interpulse spacing of τ CPMG = 10 ms, TI1 10 ms, Δ TI 130 ms, 4 dynamic scans, a Look-Locker read-out with high flip angles (95°) to ensure brain tissue saturation, and a total scan duration of 50 seconds.

Cerebral blood flow was measured in the whole brain using a 2D gradient-echo single-shot EPI pCASL sequence with the following parameters: FOV 240 x 240 x 133 mm, voxel size 3 x 3 x 7 mm, 19 slices, labelling duration 1800 ms, post-labelling delay 1800 ms, flip angle 90°, TR/TE 4400/14 ms, and a SENSE acceleration factor AP 2.5. Additional parameters were SPIR fat suppression, two background tissue suppression pulses, 140 control-label pairs, and total

scan duration of 20 minutes. The labelling plane was manually placed 90 mm below the middle slice of the imaging volume, and perpendicular to the brain feeding arteries visualized on a phase contrast MRA scout scan. Balanced pCASL labelling with flip angles of 27.81°, radio frequency interval and duration of 1.21 ms and 0.48 ms, and gradient strength average and maximum of 0.36 mT/m and 5.0 mT/m were used. A magnetization equilibrium (M0) scan was acquired for CBF quantification using the same parameters as pCASL, except that labelling and background suppression were switched off.

2.4 | Vasodilatory challenge

Following the baseline scans, an intravenous bolus of 16 mg/kg acetazolamide (dissolved in 20 mL saline, 0.9% NaCl) was infused at a flow rate of 0.1 mL/sec and flushed with 10 mL saline. The T₂-TRIR scans were repeated 25 minutes after the start of the acetazolamide injection when vasodilation has typically reached a maximum.^{35,38}

2.5 | Image analysis

Vessel stenosis was assessed in the circle of Willis vessels on MRA and vasculopathy was defined as >50% narrowing of a vessel or presence of comorbid Moyamoya. Presence of white matter hyperintensities was defined as ≥2 lesions ≥5 mm in diameter, where diameter was defined as the maximum length along a major axis of a lesion in 3D as described previously.²⁶

2.6 | SvO₂, OEF, CaO₂, DO₂ and CMRO₂ quantification

An example of the masked region of interest is shown in Figure 1C. The T₁ and T₂ were simultaneously fitted by a least-squares minimizing algorithm designed to find the combination of voxels in the sagittal sinus ROI resulting in the lowest residual error of fitted T₁ and T₂ values from the following model:

TABLE 1 Baseline characteristics and MRI parameters in healthy controls and patients with sickle cell disease

Baseline characteristic	Controls		Patients with SCD		P-value		
	(n = 11)		(n = 38)				
Age [yrs]	37.36 ± 15.43		32.08 ± 11.14		.31		
Sex	55% male		63% male		-		
Genotype	HbAA (n = 9, 82%) HbAS (n = 2, 18%)		HbSS (n = 33, 87%) HbSβ0 (n = 5, 13%)		-		
Hydroxyurea, n [%]	-		13 (37)		-		
Average dose mg/kg	-		15.88 ± 2.94		-		
Chronic blood transfusions, n [%]	-		3 (9)		-		
Vasculopathy (%)	-		1 (2)		-		
SCI status	4 (45)		31 (82)		-		
Volume of lesions [mL]	0.04 [IQR 0.54]		0.59 [IQR 2.99]				
Hematocrit [%]	42 ± 3		26 ± 4		<.001		
Hemoglobin [g/dL]	13.7 ± 1.3		8.8 ± 1.4		<.001		
HbS%	36.9 ± 0.4		80.4 ± 15.1		<.001		
HbF%	-		9.4 ± 7.6		-		
CaO ₂ [μmol O ₂ /100mL blood]	804 ± 73		515 ± 81		<.001		
MRI parameter	Baseline	Post-ACZ	Δ	Baseline	Post-ACZ	Δ	Groups
T _{1b} [s]	1.76 ± 0.09	1.69 ± 0.11	0.11	1.81 ± 0.10	1.71 ± 0.09	<0.001	.23
T _{2b} [ms]	77.6 ± 10.9	124.5 ± 22.7	<0.001	88.0 ± 13.3	115.4 ± 20.2	<0.001	.04
CBF [mL/100/min]	45.7 ± 4.8	76.2 ± 9.5	<0.001	73.9 ± 16.0	97.0 ± 17.9	<0.001	<.001
SvO ₂ [%]	64.1 ± 3.8	78.7 ± 7.0	<0.001	71.4 ± 4.3	79.4 ± 5.7	<0.001	<.001
DO ₂ [μmol O ₂ /100g/min]	368.1 ± 42.3	616.0 ± 105.3	<0.001	377.1 ± 66.8	499.4 ± 87.4	<0.001	.69
OEF [%]	35.3 ± 3.6	19.7 ± 7.1	<0.01	27.1 ± 4.4	19.0 ± 5.8	<0.001	<.001
CMRO ₂ [μmol O ₂ /100g/min]	127.2 ± 19.5	122.8 ± 43.8	0.78	101.7 ± 23.6	91.0 ± 29.5	<0.01	<.01

Bold values indicate statistical significance.

Abbreviations: ACZ, acetazolamide; SCD, sickle cell disease; CaO₂, Oxygen carrying capacity of blood was calculated from hemoglobin so does not represent a separate measure; HbS% and HbF% is reported for the n = 2 controls that had the HbAS genotype; CBF, whole brain cerebral blood flow; CMRO₂, cerebral metabolic rate of oxygen; DO₂, oxygen delivery; IQR, interquartile range; OEF, oxygen extraction fraction; SvO₂, venous oxygen saturation; T_{1b}, longitudinal relaxation time of blood; T_{2b}, transverse relaxation time of blood; Δ, within-group change after acetazolamide.

$$M(TI) = MO \left[1 - \left(1 + e^{-\frac{eTE}{T_2}} \cdot IE \right) \cdot e^{-\frac{TI}{T_1}} \right] \quad (1)$$

where M is the longitudinal magnetization of blood at each inversion recovery time (TI), MO is the equilibrium magnetization of blood, eTE is the effective echo time and IE is inversion efficiency. An example of the exponential T_1 and T_2 decay of blood within the sagittal sinus is shown in Figure 1D. The resulting T_2 values were converted to venous oxygen saturation (SvO_2) using a recently developed model,^{22,39} for sickle cell disease patients:

$$R_2 (s^{-1}) = 70 * (1 - SvO_2) + 5.75 \quad (2)$$

and for healthy controls:

$$R_2 (s^{-1}) = 77.5 * Hct * (1 - SvO_2)^2 + 27.8 * (1 - SvO_2)^2 + 6.95 * Hct + 2.34 \quad (3)$$

where $R_2 = 1/T_2$, Hct is the measured Hct. The equation was solved for venous oxygen saturation (SvO_2) in each subject before and after acetazolamide. Since arterial oxygenation (SaO_2) in the brain is similar to that in the periphery, and can be assumed to be normal in the absence of cardio-pulmonary disease, we assumed SaO_2 was equal to 0.98, or almost fully saturated. Subsequently, the oxygen extraction fraction (OEF) was calculated using the formula:

$$OEF(\%) = (SaO_2 - SvO_2) / SaO_2 * 100 \quad (4)$$

Oxygen carrying capacity (CaO_2) was calculated from measured hemoglobin (HB, g/dL) using the formula:

$$CaO_2 (\mu\text{mol } O_2 / 100\text{mL blood}) = [(HB \times 1.34 \times SaO_2) + (0.003 \times pO_2)] / 22.4 * 1000 \quad (5)$$

Where HB is hemoglobin concentration in g/100 mL obtained from blood samples, 1.34 mL/g is the constant representing the amount of oxygen that can bind to HB, 0.0031 (mL O_2 /mmHg O_2 /100 mL blood) is the solubility coefficient of oxygen in human plasma, and pO_2 in mmHg is the arterial oxygen tension of 1. Unit conversion of oxygen carrying capacity (CaO_2) to molar concentrations was performed by dividing by 22.4*1000 obtained from the gas law equation at standard temperature and pressure ($PV = nRT$, where P is pressure of 1 atm, V is volume in L, n is 1 mol, R is the ideal gas law constant of 0.08206 L atm/[mol K] and T is 273 Kelvin). One μmol at standard chemical conditions occupies 0.0224 mL, so to substitute mL O_2 for $\mu\text{mol } O_2$ in the CaO_2 equation, we divided it by 44.64 mL/ μmol . Then, $CMRO_2$ was calculated according to Fick's principle:

$$CMRO_2 (\mu\text{mol } O_2 / 100\text{g}/\text{min}) = CBF \times OEF \times CaO_2 \quad (6)$$

Finally, oxygen delivery (DO_2) was calculated by:

$$DO_2 (\mu\text{mol } O_2 / 100\text{g}/\text{min}) = CBF \times CaO_2 \quad (7)$$

The $CMRO_2$ was calculated in the whole brain (calculated from CBF in GM plus WM minus lesions Figure 1B) with CBF quantified with a two-compartment model as described previously.²⁶

2.7 | Statistical analysis

Statistical analyses were performed in R 3.4.3 (R Core Team [2017] R Foundation for Statistical Computing, Vienna, Austria). First, Shapiro-Wilk normality test was used, and subsequently Wilcoxon rank sum (significant non-normal distribution) or t test (normal distribution) for group differences. Paired tests were used to assess statistical significance of changes from baseline to post-acetazolamide conditions. $P < .05$ was considered significant. Variables were summarized by means and standard deviations. Associations between $CMRO_2$ and blood values were assessed using linear regression to determine if the slope was significantly different from zero. A Benjamini-Hochberg adjustment for family-wise error was performed to correct for multiple comparisons.

3 | RESULTS

3.1 | Participant characteristics

The baseline characteristics of the 38 patients and 11 healthy controls that were included are presented in Table 1. 14 patients were using hydroxyurea medication and three were receiving transfusions, of which two were also on hydroxyurea medication.

3.2 | Elevated venous oxygen saturation (SvO_2) in SCD

In the patient group, T_2 fitting failed in two cases. Therefore 36 patients were included in the T_2 , OEF, and $CMRO_2$ analysis. In the healthy control group, initially consisting of 11 healthy volunteers, two fits failed. The remaining fits were robust, as shown in the example in Figure 1D. The average T_2 values were higher in SCD patients compared to controls (Table 1). The corresponding SvO_2 was also higher in SCD patients ($71.4 \pm 4.2\%$) compared to healthy controls ($64.1 \pm 3.8\%$, $P < .001$). The average T_1 values did not differ between SCD patients and controls (Figure S1).

3.3 | Baseline hemodynamic results

Hemoglobin concentration was lower in patients compared to controls (8.8 ± 1.4 versus 13.7 ± 1.3 g/dL, $P < .001$), which led to a lower calculated oxygen carrying capacity (CaO_2) in patients compared to controls (515 ± 81 versus 804 ± 73 $\mu\text{mol } O_2 / 100\text{mL blood}$, $P < .001$). Oxygen delivery (DO_2) was similar in patients compared to controls

(377 ± 67 versus 367 ± 42 $\mu\text{mol O}_2/100\text{g}/\text{min}$, $P = .698$), due to compensatory elevated CBF in patients versus controls (74 ± 16 versus 46 ± 5 $\text{mL}/100\text{g}/\text{min}$, $P < .001$). In spite of the similar DO_2 , we observed lower OEF in patients compared to controls (27.1 ± 4.4 versus $35.3 \pm 3.6\%$, $P = .001$). As a result, SCD patients had lower CMRO_2 compared to controls (101.7 ± 23.6 versus 127.2 ± 19.5 $\mu\text{mol O}_2/100\text{g}/\text{min}$, $P = .005$) (Figure 2).

3.4 | Response to acetazolamide (ACZ) challenge

In order to assess if CMRO_2 in SCD patients could be normalized by vasodilation, we repeated the measurements after acetazolamide (ACZ). We observed that there was a significant increase in venous saturation (SvO_2) in both patients with SCD ($P < .001$) and in healthy controls ($P < .001$) indicating that a greater volume of oxygenated

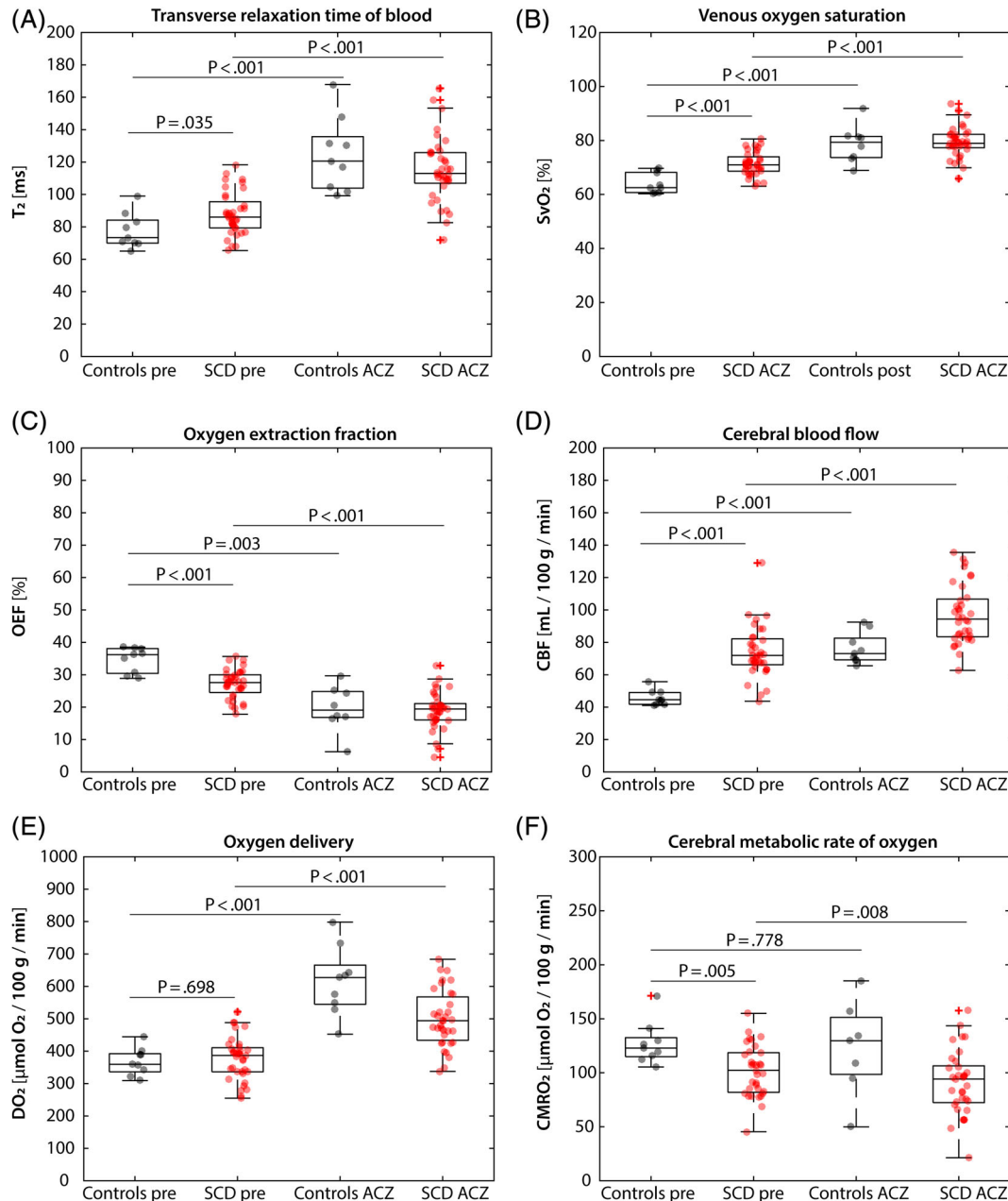


FIGURE 2 Box-plots showing the statistical differences between adults with sickle cell disease (SCD) and controls, before (pre), and after acetazolamide (ACZ) injection. A, The T_2 of blood was higher in patients with SCD at baseline and increased after ACZ in both groups. B, Venous oxygen saturation (SvO_2) was higher in patients with SCD and increased after ACZ in line with increased blood volume due to vasodilation. C, Oxygen extraction fraction (OEF) was lower in patients with SCD and declined after ACZ. D, Cerebral blood flow (CBF) in the whole brain (excluding lesions) was higher in patients with SCD and increased in both groups after ACZ. The highest CBF at baseline was in a patient with comorbid moyamoya syndrome. E, Oxygen delivery was not significantly different in patients with SCD compared to controls, and increased after ACZ due to the increase in CBF. F, CMRO_2 was lower in patients with SCD, and remained stable after ACZ in controls, but declined in patients with SCD. P -values remained significant after Benjamini-Hochberg adjustment for family-wise error. Lines and error bars indicate mean and SD [Color figure can be viewed at wileyonlinelibrary.com]

blood was delivered by the increased CBF after ACZ (Figure 2). Although the absolute change in CBF was similar in patients and controls (Δ CBF was 23 and 30 mL/100 g/min), the relative change in CBF, called cerebrovascular reserve, was lower in patients with SCD versus controls (43.1 ± 12.5 versus $67.0 \pm 20.0\%$, $P = .003$). The increase in CBF after ACZ was accompanied by a drop in OEF in patients with SCD ($P < .001$) as well as in controls ($P = .003$) (Table 1). After ACZ, $CMRO_2$ declined significantly in SCD patients (-8.4 ± 16.9 , $P = .008$). No significant decline was observed in healthy controls (-4.6 ± 41.3 , $P = .78$), due to both the lower effect size (Cohen's

$d = 0.40$ in patients and 0.13 in controls) and sample size, however it suggests that the ACZ challenge was indeed closer to isometabolic in controls than in patients.

3.5 | $CMRO_2$ associations with laboratory markers

In SCD patients, there was no significant difference in $CMRO_2$ between patients on hydroxyurea compared to patients not taking hydroxyurea ($P = .33$) (Figure S2). We found a moderate negative

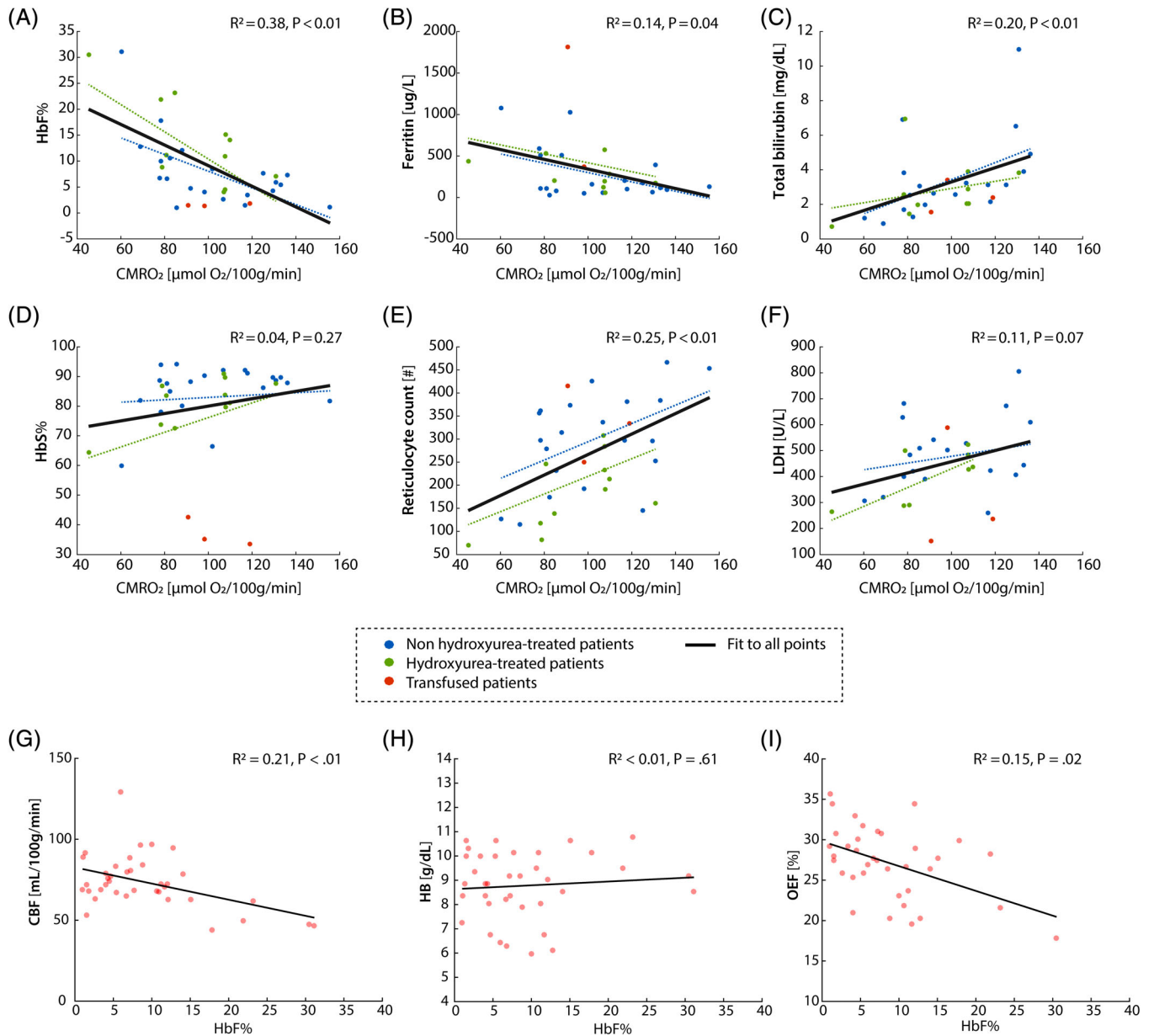


FIGURE 3 Laboratory correlates of cerebral metabolic rate of oxygen ($CMRO_2$) in adults with sickle cell disease A, HbF%, B, Ferritin, C, total bilirubin, D, HbS%, E, reticulocyte count, and F, lactate dehydrogenase (LDH). Non-hydroxyurea-treated patients are shown in blue, hydroxyurea-treated patients in green, and transfused patients in orange. The dotted colored lines show the fit for the non-hydroxyurea and hydroxyurea-treated groups, while the black solid line shows the linear fit through all patients' data points. P -values indicate significant associations. G, HbF% was inversely associated with cerebral blood flow (CBF), H, HbF% was not associated with hemoglobin concentration, I, HbF% was inversely associated with oxygen extraction fraction (OEF) [Color figure can be viewed at wileyonlinelibrary.com]

correlation between CMRO₂ and HbF% ($R^2 = 0.38, P < .01$), a significant but weak positive association between CMRO₂ and reticulocyte count ($R^2 = 0.25, P < .01$), total bilirubin ($R^2 = 0.20, P < .01$) and ferritin ($R^2 = 0.14, P = .04$). There was no association with lactate dehydrogenase ($R^2 = 0.11, P = .07$) or HbS% ($R^2 = 0.04, P = .27$) (Figure 3A-F). These *P*-values remained significant after Benjamini-Hochberg family-wise error correction. Both OEF and CBF were also inversely associated with HbF% on univariate analysis (Figure 3G,I).

3.6 | Brain anatomical features and whole-brain CMRO₂

We found no association between CMRO₂ and lesion volume in patients with SCD (Spearman's $\rho = -0.03, P = .85$), and also no statistically significant correlation between OEF and lesion volume in patients with SCD (Spearman's $\rho = -0.3, P = .07$). There was no difference in GM fraction (GM divided by total intracranial volume) between patients with SCD (mean 0.42 ± 0.05) and controls (mean $0.46 \pm 0.05, P = 0.10$). Also, there was no significant correlation between CMRO₂ and GM fraction within the patient group ($r = -0.07, P = 0.70$) or within the control group ($r = 0.47, P = 0.21$). In patients with SCD, men had higher CMRO₂ compared to women ($P < .01$). There was no significant effect of age on CMRO₂ ($P = .20$).

4 | DISCUSSION

The purpose of this study was to investigate ischemic risk in SCD patients by assessing CMRO₂ and its response to increased flow upon vasodilation with acetazolamide. We used ASL and T₂-TRIR MRI with a recently introduced SCD-specific model to non-invasively measure CBF and cerebral SvO₂. Our observations support our hypothesis that SCD patients have reduced OEF and CMRO₂. This indicates that in SCD, CMRO₂, and therefore also neuronal function, has adapted to lower oxygen availability. Our second hypothesis was that acetazolamide would normalize CMRO₂ by increasing oxygen delivery (DO₂), but our observations do not support this hypothesis and instead show that DO₂ was normal in SCD patients, and that OEF and CMRO₂ declined after acetazolamide. The higher SvO₂ after acetazolamide suggests that arterial blood shunted directly to the venous side without oxygen extraction by the brain tissue, resulting in a reduced OEF and subsequently also reduced CMRO₂. Our observations suggest a potentially impaired distribution of oxygen even when blood flow is artificially increased with acetazolamide, perhaps due to differences in resistance of healthy and diseased vascular beds.

4.1 | Reduced oxygen utilization despite normal oxygen delivery

Previous studies using nitrous oxide have also shown reduced cerebral oxygen utilization in SCD and other anemias.^{40,41} PET is the gold

standard for CBF, OEF and CMRO₂, and an early study in SCD patients found that CBF was appropriately elevated in the cortical MCA territory to conserve normal DO₂ and average CMRO₂ compared to controls.⁵ In the PET study, half of the patients had CMRO₂ values below the lowest CMRO₂ value of controls but on average the groups did not differ. We also found no difference in DO₂ between patients and controls due to elevated CBF as previously reported for whole-brain and GM.^{23,29}

4.2 | Higher venous saturation

We found higher T₂ in patients with SCD in our study, which denotes increased venous oxygen saturation (SvO₂),⁴² and is in agreement with recent reports of increased SvO₂ in children and adults with SCD using T₂-TRUST as well as susceptibility MRI,^{21,22,43} but in contrast to other reports⁴⁴ which differ due to differences in the choice of calibration model. Nevertheless, elevated SvO₂ in SCD may indicate impaired oxygen extraction as has been reported in the peripheral tissue⁴⁵ and may explain the high risk of tissue hypoxia as well as infarction in SCD.

4.3 | Reduced oxygen extraction fraction

We observed reduced OEF in adults with SCD with an MR technique that measures post-capillary venous OEF,³³ which is spatially and temporally different from the ASE technique which measures OEF locally in deep WM tissue and has found elevated OEF in children with SCD.^{27,28,46} Fields, Guilliams, Ford and colleagues consistently find increased OEF in the deep WM tissue, which, in steno-occlusive disease, reflects stage 2 hemodynamic compromise when OEF starts to compensate for critically low CBF to try to maintain DO₂.⁴⁷ In children with SCD, this increased OEF in WM may indicate that compensatory mechanisms are activated to maintain CMRO₂. Reduced OEF in whole brain in adults with SCD may indicate that hemodynamic compromise has not reached a critical level, or that our globally measured SvO₂, OEF, and CMRO₂ were dominated by the metabolic activity of the GM, which may be stealing from the WM. Indeed, CBF might preferentially be distributed to maintain DO₂ in the GM, where many neuronal processes must be fed, by using the cerebrovascular reserve that is still available, and hence keeping OEF normal, as others have found using global venous techniques.^{22,23}

4.4 | Homeostatic relationship between CBF and OEF after acetazolamide

If the low CMRO₂ were just the result of flow limitation, acetazolamide would be expected to ameliorate the reduced metabolism in SCD patients by dilating the vessels and increasing delivery of oxygenated blood. As anticipated, CBF increased and OEF declined in both groups in response to acetazolamide.⁴⁸ There was no change

detected in CMRO₂ in healthy controls which is supported by a previous study using susceptometry-based oximetry with hypercapnia challenge.⁴⁹ Interestingly, we observed a small reduction in CMRO₂ in patients with SCD, indicating a mismatch between CBF and OEF. A power analysis showed that there was 95% power to detect a reduction in the SCD group, while there was 10% power in the control group due to the lower sample size. Normalizing CBF and increasing oxygen carrying capacity with transfusions could shed light on a potential mechanism explaining this mismatch. However, studies on children with SCD addressing acute effects of transfusions on global or regional OEF and CMRO₂ have not found significant changes in CMRO₂, possibly due to sufficiently elevated compensatory CBF before transfusion.^{46,50} An alternative explanation for the drop in CMRO₂ is that carbonic anhydrase inhibition with acetazolamide may influence the Hb-O₂ dissociation curve due to the increased acidotic environment, leading to tighter Hb-O₂ binding and lower OEF and CMRO₂.

4.5 | Heterogeneous oxygen distribution after acetazolamide

The ability of vessels to dilate will govern their vascular resistance which will determine the favorable dispersal of blood towards healthier vascular beds. This would suggest that there exists heterogeneity in the blood flow distributed to different vascular beds, and could explain the preferential localization of ischemic lesions in specific low-flow areas.²⁷ It is known that blood arrival times are heterogeneous due to the anatomic architecture of the cerebral vessels,⁵¹ but downstream capillary transit times may also reflect certain regional differences. For instance, recent work has shown that heterogenous blood distribution can lead to reduced OEF and CMRO₂ in the presence or introduction of increased transit time heterogeneity,^{30,52} which could be an explanation for why we found lower OEF and CMRO₂ after acetazolamide. Acetazolamide would induce dilation only in healthy vessels which are able to dilate, leading to lower resistance and more blood flow. For diseased vessels, acetazolamide would have little effect, leading to no or little change in blood flow and hence no change in oxygen delivery. The surplus oxygen is delivered to healthy vascular beds due to lower resistance, but have neither the additional oxygen requirement nor a sufficient oxygen diffusion gradient for oxygen to unload, so oxygen flows to the venous side (we found increased SvO₂). Hence, reduced CMRO₂ might only occur if there exists a heterogeneity in the ability of different vascular beds to dilate. We cannot exclude the possibility that chronically anemic patients may also lose capillary surface area through vascular remodeling; but the imaging used in this study cannot quantify vascular surface area.

4.6 | CMRO₂ and ischemic risk

In this study there was no association between CMRO₂ and lesion volume contrary to what has been reported in patients with multiple

sclerosis.⁵³ We observed a higher prevalence of lesions in the WM where CBF is low, and recent studies show that although OEF may be elevated in children in these locations,^{27,28} CMRO₂ is primarily high in more physiologically active GM.⁵⁴ Global CMRO₂ measurements may not reflect local changes in metabolism, so regional measurements may better identify areas of particular risk for SCIs. Hence, the lack of association between global CMRO₂ and lesion volumes in WM can be explained by the high CBF in GM, masking the reduced CMRO₂ in areas with lesions. The role of oxygenation in the development and progression of lesions is particularly challenging to study, because lesions are not detected at the time they occur, and can therefore represent periods of acute anemia experienced a long time before lesion detection with MRI. So, the lack of association between CMRO₂ and lesions in our study does not necessarily mean that there is no relationship, but rather that our cross-sectional design was poorly suited to detect it, and longitudinal studies following young patients into adulthood would be insightful in this respect.

4.7 | CMRO₂ and HbF

We found that CMRO₂ was inversely associated with HbF, which was not found by Herold *et al.*⁵ In univariate analyses, Fields *et al.* recently found that SCD patients with higher HbF levels also had lower OEF in a comparison between patients treated with hydroxyurea and not treated with hydroxyurea.⁵⁵ This is not surprising if OEF elevations are related to disease severity as they suggest, but would be surprising if OEF elevations are related to improved oxygen extraction. If higher HbF is associated with low oxygen extraction fraction, then this could suggest that HbF has a tighter Hb-O₂ binding affinity, leading to less efficient oxygen unloading. Finally, the inverse relationship between CBF and HbF is supported by literature in sickle cell mice,⁵⁶ which Cui *et al.*⁵⁶ suggest may be related to lower sickling, reduced oxidative stress, improved NO activity or improved oxygen carrying capacity and delivery. Thus, the balance between oxygen delivery and extraction may be perturbed in the presence of HbF whereby more oxygen is delivered than can be extracted. Furthermore, as discussed above, variations in capillary transit time and shunting may mean that there is less time and insufficient oxygen diffusion gradient to unload oxygen resulting in a lower global OEF and subsequently lower global CMRO₂. Together, our findings suggest that reduced CMRO₂ could partly be mediated by the effect of higher HbF levels on both OEF and CBF. However, the HbF correlation with CMRO₂ was from univariate analysis, and future studies with larger cohorts will likely show that the effects of HbF on CMRO₂ are mitigated by covariation with HbA, so the driving factor in predicting CMRO₂ requires further investigation.

4.8 | Limitations

A general limitation of MRI-derived CMRO₂ is error propagation of the individual measurements of CBF, OEF and CaO₂ due to multiplication.⁵⁷ While there is currently no direct MRI-CMRO₂ measurement,

we attempted to reduce errors in CBF by correcting for differences in T1 of blood, arterial transit time and labeling efficiency.²⁶ Another limitation of CMRO₂ calculation from T₂-TRIR MRI is the reliance on a model to obtain OEF values. A recent study has highlighted the importance of model choice in calculating SvO₂ (and subsequent OEF), which can explain the observed differences of elevated,^{21,28,44,46,50} reduced,²² or unchanged^{21,23} CMRO₂ in patients with SCD. Until recently, two models were available for T₂-derived SvO₂; the first was calibrated in bovine blood in a wide range of Hct (35–55%) considered to be a healthy range,^{58,59} and the second was calibrated in human sickle cell blood in a slightly smaller but more appropriate range of Hct for anemia of 24–40%.²² The bovine model shows higher OEF in SCD (lower SvO₂) compared to controls,^{21,44} but it should be noted that the model is biased at low Hct. On the other hand, the sickle cell model previously showed lower OEF in SCD (higher SvO₂) compared to controls,²² a finding that is supported here and also by an independent susceptibility MRI study showing higher SvO₂ in SCD compared to controls.⁴³ The main difference between the sickle-cell model and healthy human blood model is that the sickle-cell model does not show dependence on Hct which is most probably due to the narrow range of Hct used for calibration or that Hct is too low to influence the measured T₂ value. A recent approach has used subject-specific calibration resulting in OEF similar to the sickle-cell model.²³ Although validation of the models in SCD is still warranted by comparison with PET, which is the current gold standard for OEF and CMRO₂ measurements, our choice for the sickle cell model is justified by the fact that it was calibrated over a relevant hematocrit range for our population. We assumed arterial oxygen saturation to be 0.98 which may have been inaccurate in SCD patients, but given the median saturation of 0.97 measured clinically in two studies including more than 100 children and 89 adults with SCD in steady-state respectively^{60,61} we expect that any resulting error in SaO₂ and CaO₂ will be small, particularly because we did not include patients with proven pulmonary hypertension or severe cardiomyopathy, both of which may result in low arterial saturation.

5 | CONCLUSION

In this study, we used T₂-TRIR and ASL MRI to measure reduced CMRO₂ in adults with SCD. Overall, oxygen delivery to the brain was normal in SCD patients. However, specific capillary beds may have adapted to chronic low oxygen delivery due to anemia as differences in dilatory capacity and resistance may arise depending on metabolic requirements. We conclude firstly that CMRO₂ does not improve in response to transient changes in oxygen availability induced by acetazolamide in SCD patients, despite the increase in CBF, and secondly, that this worsening CMRO₂ in SCD patients may be due to increased capillary transit time heterogeneity exacerbated by high flow.^{30,52}

ACKNOWLEDGEMENTS

The authors would like to thank all the participants for their time and effort to take part in this study.

Funding: Fonds Nuts Ohra grant no. 1303-055.

Trial registration: ClinicalTrials.gov ID: NCT02824406.

CONFLICT OF INTEREST

The authors declare no competing financial interests.

AUTHOR CONTRIBUTIONS

L.V. and B.J.B. recruited and scanned the participants, and wrote the manuscript. E.T.P. developed and implemented the T2-TRIR sequence and analysis software to fit the T2 data. H.J.M.M.M. wrote the analysis software for the ExploreASL toolbox. J.P. performed pre-processing analysis of ASL images to remove an artifact using principal components analysis. C.B.M. performed radiologic assessment of MRA and FLAIR data. E.T.P., E.vB., A.J.N., and B.J.B. analyzed and interpreted the data. All authors reviewed the manuscript.

ORCID

Lena Václavů  <https://orcid.org/0000-0001-8617-7752>

REFERENCES

- Dowling M, Quinn C, Plumb P, et al. Acute silent cerebral infarction occurs during acute anemic events in children with and without sickle cell disease. *Blood*. 2012;120(19):3891-3897.
- Dlamini N, Saunders DE, Bynevelt M, et al. Nocturnal oxyhemoglobin desaturation and arteriopathy in a pediatric sickle cell disease cohort. *Neurology*. 2017;89:1-7.
- Kirkham FJ, Hewes DKM, Prengler M, Wade A, Lane R, Evans JPM. Nocturnal hypoxaemia and central-nervous-system events in sickle-cell disease. *Lancet*. 2001;357(9269):1656-1659.
- Prohovnik I, Pavlakis SG, Piomelli S, et al. Cerebral hyperemia, stroke, and transfusion in sickle cell disease. *Neurology*. 1989;36(3):344.
- Herold S, Brozovic M, Gibbs J, et al. Measurement of regional cerebral blood flow, blood volume and oxygen metabolism in patients with sickle cell disease using positron emission tomography. *Stroke*. 1986;17(4):692-698.
- Gevers S, Nederveen AJ, Fijnvandraat K, et al. Arterial spin labeling measurement of cerebral perfusion in children with sickle cell disease. *J Magn Reson Imaging*. 2012;35(4):779-787.
- Lee JM, Vo KD, An H, et al. Magnetic resonance cerebral metabolic rate of oxygen utilization in hyperacute stroke patients. *Ann Neurol*. 2003;53(2):227-232.
- Debaun MR, Kirkham FJ. Central nervous system complications and management in sickle cell disease. *Blood*. 2016;127(7):829-838.
- Adams RJ, McKie VC, Hsu L, et al. Prevention of a first stroke by transfusions in children with sickle cell anemia and abnormal results on transcranial Doppler ultrasonography. *N Engl J Med*. 1998;339(1):5-11.
- Van Der Land V, Zwanenburg JJM, Fijnvandraat K, et al. Cerebral lesions on 7 Tesla MRI in patients with sickle cell anemia. *Cerebrovasc Dis*. 2015;39(3-4):181-189.
- Jordan LC, Kassim AA, Donahue MJ, et al. Silent infarct is a risk factor for infarct recurrence in adults with sickle cell anemia. *Neurology*. 2018;00:e1-e4.
- Steen RG, Miles MA, Helton KJ, et al. Cognitive impairment in children with hemoglobin SS sickle cell disease: relationship to MR imaging findings and hematocrit. *AJNR Am J Neuroradiol*. 2003;24(3):382-389.
- van der Land V, Hijmans CT, de Ruiter M, et al. Volume of white matter hyperintensities is an independent predictor of intelligence quotient and processing speed in children with sickle cell disease. *Br J Haematol*. 2015;168(4):553-556.
- Biagi L, Abbruzzese A, Bianchi MC, Alsop DC, del Guerra A, Tosetti M. Age dependence of cerebral perfusion assessed by magnetic resonance continuous arterial spin labeling. *J Magn Reson Imaging*. 2007;25(4):696-702.

15. Ohene-Frempong K, Weiner SJ, Sleeper LA, et al. Cerebrovascular accidents in sickle cell disease: rates and risk factors. *Blood*. 1998;91(1):288-294.
16. Prohovnik I, Hurler-Jensen A, Adams R, De Vivo D, Pavlakis SG. Hemodynamic etiology of elevated flow velocity and stroke in sickle-cell disease. *J Cereb Blood Flow Metab*. 2009;29:803-810.
17. Adams R, McKie V, Nichols F, et al. The use of transcranial ultrasonography to predict stroke in sickle cell disease. *N Engl J Med*. 1992;9:605-610.
18. Kety SS. Human cerebral blood flow and oxygen consumption as related to aging. *J Chronic Dis*. 1956;3(5):478-486.
19. De Vis JB, Hendrikse J, Bhogal A, et al. Age-related changes in brain hemodynamics: a calibrated MRI study. *Hum Brain Mapp*. 2015;36(10):3973-3987.
20. Derdeyn CP, Grubb RL, Powers WJ. Cerebral hemodynamic impairment: methods of measurement and association with stroke risk. *Neurology*. 1999;53(2):251-251, 259.
21. Jordan LC, Gindville MC, Scott AO, et al. Non-invasive imaging of oxygen extraction fraction in adults with sickle cell anaemia. *Brain*. 2016;139(3):1-13.
22. Bush AM, Coates TD, Wood JC. Diminished cerebral oxygen extraction and metabolic rate in sickle cell disease using T2 relaxation under spin tagging MRI. *Magn Reson Med*. 2018;80(1):294-303.
23. Li W, Lu H, Xu X, van Zijl PCM. Quantification of whole - brain oxygenation extraction fraction and cerebral metabolic rate of oxygen consumption in adults with sickle cell anemia using individual T 2 - based oxygenation calibrations. *Magn Reson Med*. 2020;83(3):1066-1080.
24. Nur E, Kim Y-S, Truijen J, et al. Cerebrovascular reserve capacity is impaired in patients with sickle cell disease. *Blood*. 2009;114(16):3473-3478.
25. Kosinski PD, Croal PL, Leung J, et al. The severity of anaemia depletes cerebrovascular dilatory reserve in children with sickle cell disease: a quantitative magnetic resonance imaging study. *Br J Haematol*. 2017;176(2):280-287.
26. Václavů L, Meynart BN, Mutsaerts HJ, et al. Hemodynamic provocation with acetazolamide shows impaired cerebrovascular reserve in adults with sickle cell disease. *Haematologica*. 2019;104(4):690-699.
27. Ford AL, Ragan DK, Fellah S, et al. Silent infarcts in sickle cell anemia occur in the borderzone region and are associated with low cerebral blood flow. *Blood*. 2018;132(16):1714-1723.
28. Fields ME, Guilliams KP, Ragan DK, et al. Regional oxygen extraction predicts border zone vulnerability to stroke in sickle cell disease. *Neurology*. 2018;90(13):e1134-e1142.
29. Chai Y, Bush AM, Coloigner J, et al. White matter has impaired resting oxygen delivery in sickle cell patients. *Am J Hematol*. 2019;94(4):467-474.
30. Angleys H, Østergaard L, Jespersen SN. The effects of capillary transit time heterogeneity (CTH) on brain oxygenation. *J Cereb Blood Flow Metab*. 2015;35(5):806-817.
31. DeBaun MR, Armstrong FD, McKinstry RC, et al. Silent cerebral infarcts: a review on a prevalent and progressive cause of neurological injury in sickle cell anemia Silent cerebral infarcts: a review on a prevalent and progressive cause of neurological injury in sickle cell anemia Department of Pedia. *Blood*. 2012;119(20):4587-4597.
32. Xu F, Ge Y, Lu H. Noninvasive quantification of whole-brain cerebral metabolic rate of oxygen (CMRO2) by MRI. *Magn Reson Med*. 2009;62(1):141-148.
33. De Vis JB, Petersen ET, Alderliesten T, et al. Non-invasive MRI measurements of venous oxygenation, oxygen extraction fraction and oxygen consumption in neonates. *Neuroimage*. 2014;95:185-192.
34. Petersen ET, De Vis J, Alderliesten T, et al. Simultaneous OEF and haematocrit assessment using T2 prepared blood relaxation imaging with inversion recovery. *Proc Intl Soc Mag Reson Med*. 2012;20:472.
35. Vorstrup S, Henriksen L, Paulson OB. Effect of acetazolamide on cerebral blood flow and cerebral metabolic rate for oxygen. *J Clin Invest*. 1984;74(11):1634-1639.
36. Okazawa H, Yamauchi H, Sugimoto K, Toyoda H, Kishibe Y, Takahashi M. Effects of acetazolamide on cerebral blood flow, blood volume, and oxygen metabolism: a positron emission tomography study with healthy volunteers. *J Cereb Blood Flow Metab*. 2001;21(12):1472-1479.
37. Alderliesten T, De Vis JB, Lemmers PM, et al. Brain oxygen saturation assessment in neonates using T 2-prepared blood imaging of oxygen saturation and near-infrared spectroscopy. *J Cereb Blood Flow Metab*. 2017;37(3):902-913.
38. Hartkamp NS, Hendrikse J, van der Worp HB, de Borst GJ, Bokkers RPH. Time course of vascular reactivity using repeated phase-contrast MR angiography in patients with carotid artery stenosis. *Stroke*. 2012;43(2):553-556.
39. Bush A, Borzage M, Detterich J, et al. Empirical model of human blood transverse relaxation at 3 T improves MRI T2 oximetry. *Magn Reson Med*. 2017;77(6):2364-2371.
40. Heyman BA, Patterson JL, Duke TW. Cerebral circulation and metabolism in sickle cell and other chronic anemias, with observations on the effects of oxygen inhalation. *J Clin Invest*. 1952;31(9):824-828.
41. Scheinberg P. Cerebral blood flow and metabolism in pernicious anemia. *Blood*. 1951;6(3):213-227.
42. Thulborn KR, Waterton JC, Matthews PM, Radda GK. Oxygenation dependence of the transverse relaxation time of water protons in whole blood at high field. *Biochim Biophys Acta*. 1982;714(2):265-270.
43. Croal PL, Leung J, Phillips CL, Serafin MG, Kassner A. Quantification of pathophysiological alterations in venous oxygen saturation: a comparison of global MR susceptometry techniques. *Magn Reson Imaging*. 2019;58(5):18-23.
44. Watchmaker JM, Juttukonda MR, Davis LT, et al. Hemodynamic mechanisms underlying elevated oxygen extraction fraction (OEF) in moyamoya and sickle cell anemia patients. *J Cereb Blood Flow Metab*. 2016;38(9):1618-1630.
45. Nahavandi M, Millis RM, Tavakkoli F, et al. Arterialization of peripheral venous blood in sickle cell disease. *J Natl Med Assoc*. 2002;94(5):320-326.
46. Guilliams KP, Fields ME, Ragan DK, et al. Red cell exchange transfusions lower cerebral blood flow and oxygen extraction fraction in pediatric sickle cell anemia. *Blood*. 2018;131(9):1012-1021.
47. Gupta A, Baradaran H, Schweitzer AD, et al. Oxygen extraction fraction and stroke risk in patients with carotid stenosis or occlusion: a systematic review and meta-analysis. *Am J Neuroradiol*. 2014;35(2):250-255.
48. Leatherday C, Dehkharghani S, Nahab F, et al. Cerebral MR oximetry during acetazolamide augmentation: beyond cerebrovascular reactivity in hemodynamic failure. *J Magn Reson Imaging*. 2019;50(1):175-182.
49. Rodgers ZB, Englund EK, Langham MC, Magland JF, Wehri FW. Rapid T2- and susceptometry-based CMRO2 quantification with interleaved TRUST (ITRUST). *Neuroimage*. 2015;106:441-450.
50. Juttukonda MR, Lee CA, Patel NJ, et al. Differential cerebral hemometabolic responses to blood transfusions in adults and children with sickle cell anemia. *J Magn Reson Imaging*. 2019;49(2):466-477.
51. Hendrikse J, Petersen ET, van Laar PJ, Golay X. Cerebral border zones between distal end branches of intracranial arteries: MR imaging. *Radiology*. 2008;246:572-580.
52. Rasmussen PM, Jespersen SN, Østergaard L. The effects of transit time heterogeneity on brain oxygenation during rest and functional activation. *J Cereb Blood Flow Metab*. 2015;35(3):432-442.
53. Ge Y, Zhang Z, Lu H, et al. Characterizing brain oxygen metabolism in patients with multiple sclerosis with T2-relaxation-under-spin-tagging MRI. *J Cereb Blood Flow Metab*. 2012;32(3):403-412.

54. Ibaraki M, Miura S, Shimosegawa E, et al. Quantification of cerebral blood flow and oxygen metabolism with 3-dimensional PET and 15O: validation by comparison with 2-dimensional PET. *J Nucl Med.* 2007; 49(1):50-59.
55. Fields ME, Williams KP, Ragan D, et al. Hydroxyurea reduces cerebral metabolic stress in patients with sickle cell anemia. *Blood.* 2019;133(22):2436-2444.
56. Cui MH, Billett HH, Suzuka S, et al. Fetal hemoglobin improves cerebral blood flow and decreases brain inflammation in transgenic- sickle mice. *Blood.* 2016;128(22):3639-3639.
57. Merola A, Germuska MA, Murphy K, Wise RG. Assessing the repeatability of absolute CMRO₂, OEF and haemodynamic measurements from calibrated fMRI. *Neuroimage.* 2018;173: 113-126.
58. Lu H, Xu F, Grgac K, Liu P, Qin Q, van Zijl P. Calibration and validation of TRUST MRI for the estimation of cerebral blood oxygenation. *Magn Reson Med.* 2012;67(1):42-49.
59. Lu H, Ge Y. Quantitative evaluation of oxygenation in venous vessels using T2-relaxation-under-spin-tagging MRI. *Magn Reson Med.* 2008; 60(2):357-363.
60. Quinn CT, Variste J, Dowling MM. Haemoglobin oxygen saturation is a determinant of cerebral artery blood flow velocity in children with sickle cell anaemia. *Br J Haematol.* 2009;145(4):500-505.
61. Brodsky MA, Rodeghier M, Sanger M, et al. Risk factors for 30-day readmission in adults with sickle cell disease. *Am J Med.* 2017;130(5): 601.e9-601.e15.

How to cite this article: Václavů L, Petr J, Petersen ET, et al. Cerebral oxygen metabolism in adults with sickle cell disease. *Am J Hematol.* 2020;95:401-412. <https://doi.org/10.1002/ajh.25727>